Similar spectra were obtained in the ν(C–C) and ν(C–H) regions for all surfaces, suggesting that disordering induced by surface roughness is most easily accommodated by disruption of van der Waals bonding near the S end of the molecule.

Acknowledgment. We are grateful for support of this work by the National Science Foundation (CHE-8614955). Helpful discussions with Dr. Marc D. Porter are also gratefully acknowledged.

Registry No. Au, 7440-57-5; $CH_3(CH_2)_3SH$, 109-79-5; $CH_3(CH_2)_4SH$, 110-66-7; $CH_3(CH_2)_5SH$, 111-31-9; $CH_3(CH_2)_7SH$, 94805-33-1; $CH_3(CH_2)_8SH$, 1455-21-6; $CH_3(CH_2)_{11}SH$, 1322-36-7; $CH_3(CH_2)_{17}SH$, 2885-00-9.

An ab Initio Study (6-31G*) of Transition States in Glycoside Hydrolysis Based on Axial and Equatorial 2-Methoxytetrahydropyrans[1]

C. Webster Andrews,[†,2a] Bert Fraser-Reid,*[,†] and J. Phillip Bowen[‡,2b]

Contribution from the Paul M. Gross Chemical Laboratory, Department of Chemistry, Duke University, Durham, North Carolina 27706, and Laboratory for Molecular Modeling, Division of Medicinal Chemistry and Natural Products, School of Pharmacy, University of North Carolina at Chapel Hill, Chapel Hill, North Carolina 27599. *Received May 6, 1991*

Abstract: An ab initio study of proton-induced cleavage of α and β glycopyranosides has been carried out at the 6-31G* level using protonated axial and equatorial methoxytetrahydropyran as models. The conformational changes along the reaction pathway can be monitored by focusing on the C_5O_5–C_1C_2 dihedral angle, ω, which is +60° in the $^4C_1$ chair, and −60° in the $^{1,4}B$ boat. We have obtained the energy profiles of each protonated anomer for values of ω from −60° to +60°, and used these to select the most probable species that will proceed to the transition state. On the basis of least motion considerations, species in which $\omega = 0°$ are chosen on geometric grounds since the cleavage product, the cyclic oxocarbenium ion, is planar in the C_5O_5–C_1C_2 region. Additionally, low-energy conformers are considered possible precursors on the basis of energetic considerations. Stretching of the C_1–O_1 bonds of the plausible candidates then leads to the transition state. With respect to the cyclic oxocarbenium ion, a $\omega = 0°$ angle can be accommodated by several conformers, and the geometries and energies of these were evaluated. For the protonated axial anomer, the preferred intermediates are a flattened chair ($\omega = +37°$), the $^0S_2$ boat, and the E_3 endo sofa. The first and third proceed to a half-chair transition state and thence to a half-chair oxocarbenium ion. The second proceeds to a transition state and oxocarbenium ion having $B_{2,5}$ boat structure and is found to be less favorable on the basis of energetic considerations. For the protonated equatorial anomer, the favored intermediates all proceed to a ^4E endo sofa transition state, and thence to an oxocarbenium ion of the same geometry. Thus, the α and β anomers of the glycopyranosides are hydrolyzed through different retinues of intermediates and transition-state structures, and proceed to different cyclic oxocarbenium ions.

Introduction

Replacement reactions at the anomeric center (e.g., **1** → **6**) are critical events in a wide variety of biological and chemical processes, and hence they have been subjected to extensive mechanistic investigations.[3] The substrates of greatest interest are oligosaccharides, and these are comprised (mainly) of glycopyranosidic residues. Since these glycosides, e.g., **1**, are acetals and therefore acid sensitive, mechanistic investigations have traditionally employed acid-catalyzed procedures,[4] and the weight of evidence is that protonation occurs on the exocyclic oxygen,[5,6] thereby triggering formation of the cyclic oxocarbenium ion (**1** → **2** → **3**, Scheme I).

Our recent discovery that *n*-pentenyl glycosides, e.g., **5**, could be "oxidatively hydrolyzed"[9] enabled us to gain access to the key intermediate **3** under neutral conditions. This capability paved the way for us to gain insight into the stereoelectronic requirements for glycoside cleavage and establish,[10] inter alia, that intermediate $^{1,4}B$ boat conformations were specifically excluded. These results prompted us to undertake[11] an ab initio study of acetal protonation based on the simplest member of that functional class, dimethoxymethane (**7**). This study revealed that protonation evokes profound changes in the geometric and energy relationships of various acetal conformations. For example, antiperiplanar *and* synperiplanar relationships between a lone pair and the protonated aglycon were *both* found to be stabilizing.[12]

Scheme I

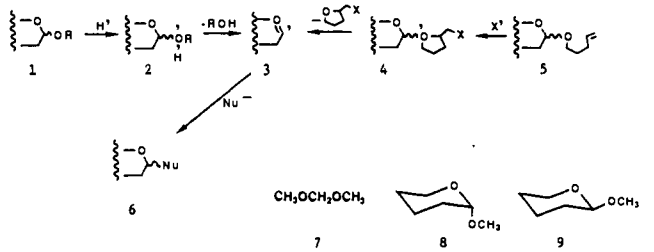

[†] Duke University.
[‡] University of North Carolina at Chapel Hill.

(1) This work was supported by grants from the National Science Foundation to B.F.-R. (CHE 8703916 and UTE 89 20033).
(2) (a) Taken from the Ph.D. Thesis of C.W.A., Duke University, 1989. Present address: Burroughs Wellcome Company, 3030 Cornwallis Road, Research Triangle Park, NC 27709. (b) Current address: Department of Chemistry, University of Georgia, Athens, GA 30602.
(3) For recent reviews, see: Sinnott, M. L. *Adv. Phys. Org. Chem.* **1988**, *24*, 113. Kirby, A. J. *Acc. Chem. Res.* **1985**, *17*, 305.
(4) Capon, B. *Chem. Rev.* **1969**, *69*, 40.
(5) Cleavage of glycosides is believed to occur via specific acid catalysis, indicating that the glycoside–proton bond is fully formed in the transition state. Bunton, C. A.; Lewis, T. A.; Llewellyn, D. R.; Vernon, C. A. *J. Chem. Soc.* **1955**, 4419. Banks, B. E. C.; Meinwald, Y.; Rhind-Tutt, A. J.; Sheft, L.; Vernon, C. A. *J. Chem. Soc.* **1961**, 3240.

0002-7863/91/1513-8293$02.50/0

Scheme II[a]

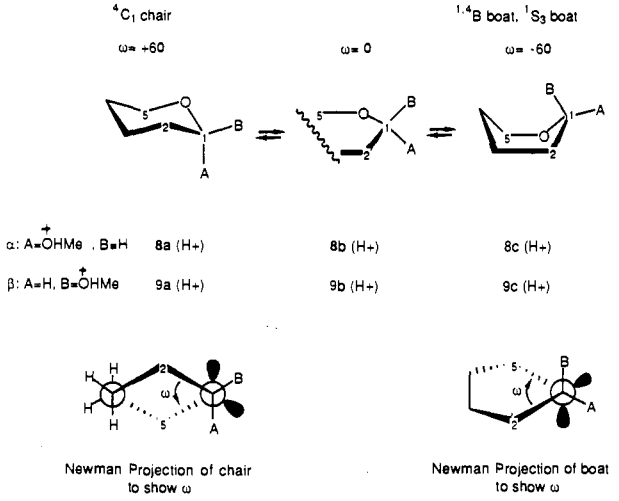

[a] See ref 29.

These conclusions have implications for the cleavage of α and β pyranosides, and hence we have extended our ab initio study to the axial and equatorial forms of methoxytetrahydropyran (MeOTHP), **8** and **9**, as models of α and β glycopyranosides, respectively.

Objectives

The dimethoxymethane study showed that protonation drives an acetal toward cleavage, and hence *protonated* anomers **8**(H^+) and **9**(H^+), Scheme II, were chosen as model precursors to cleavage. Our approach focused attention on the C_5O_5–C_1C_2 dihedral angle, ω, which ranges from +60° in the $^4C_1$ chairs **8a**(H^+) and **9a**(H^+) to −60° in the $^{1,4}B$ boats **8c**(H^+)′ and **9c**(H^+)′ (Scheme II). Conformational interconversion from $^4C_1$ chairs to $^{1,4}B$ boats passes through 0°, and the conformations of the protonated MeOTHP's clustered around this point are therefore geometrically related to the cleavage product cyclic oxocarbenium ion **3**, where ω is close to 0° (vide infra). *Angles lying between +60° and 0° therefore reflect cleavage originating from chairlike conformations, while angles between −60° and 0° reflect cleavage originating with boatlike counterparts.*

Our objective was to find the transition state(s) for cleavage, and the low-energy protonated precursors thereof. This would reveal the most probable reaction path(s).

Conformational Screening

In order to make the problem manageable computationally, we divided the ω-range into five points, +60°, +30°, 0°, −30°, and −60°, and searched for low-energy conformations at each point. The number of conformational species to be evaluated at each value of ω was reduced by application of two selection rules: (i) Starting with a $^4C_1$ chair, we focused attention on those conformers where the C5–CH_2OH group of a hexopyranose would be equatorial. This criterion follows from the *A* values obtained by Eliel.[13] (ii) Since there can be several possible conformers for any given value of ω, we applied the principles of conventional conformational analysis to choose between the various alternatives. However, where a clear favorite was not revealed by this preselection, energetic analysis was used to determine the low-energy species (vide infra).

Scheme III. Pseudorotational Boat (*B*) and Twist Boat (*S*) Conformers Having the C_5–CH_2OH (R) in Pseudoequatorial Orientation[a] (Values of ω Are Shown in Parenthesis)[d]

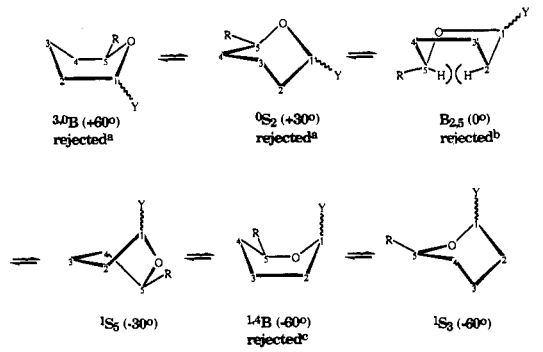

[a] In favor of chair alternatives. [b] Because of steric interactions. [c] Changes to $^1S_3$ during optimization. [d] See ref 29.

Scheme IV. Some Conformational Isomers of Oxocarbenium Ions and Protonated Methoxytetrahydropyrans (i.e., **8b**(H^+) or **9b**(H^+)) Where the C_5O_5–C_1C_2 Dihedral Angle[a] ω = 0° (6-31G*//3-21G Energies)

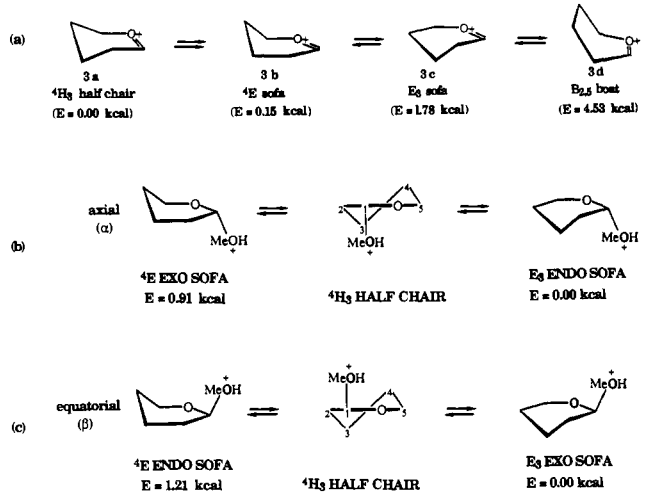

[a] See ref 29.

Boat Conformations. There are six boats (*B*) and six twist boats (*S*) in the pseudorotational itinerary of a pyranoside ring.[14] However, application of selection rule i reduces the number to the six shown in Scheme III.

Within this group, the $^{3,0}B$ form has the same dihedral angle, ω, as the $^4C_1$ chair (i.e., +60°), but if we now apply selection rule ii, the former is rejected since boats are usually less stable than chairs. Similarly all boats with ω-values lying between 0° and +60° (e.g., $^0S_2$ where ω = +30°) will have chair alternatives that will be lower in energy.

The $B_{2,5}$ boat is one of the possible ω = 0° conformers to be discussed below (see Scheme III). It is destabilized by a severe flagpole interaction between the C_2 and C_5 substituents, and was therefore rejected. Thus, only the $^1S_5$, $^{1,4}B$, and $^1S_3$ boats remain for further consideration. $^{1,4}B$ and $^1S_3$ conformers are seen to have the same ω value, but the latter, being a skew boat, should have

(6) Although the thorny issue of ring oxygen protonation[7] has recently been resurrected in a number of widely differing studies,[8] in this manuscript we confine our attention to protonation of the glycoside oxygen in view of its widespread acceptance.[4] Our studies on endo protonation are underway and will be reported in due course.

(7) Lemieux, R. U. *Adv. Carbohydr. Chem.* **1954**, 91.

(8) Post, C. B.; Karplus, M. *J. Am. Chem. Soc.* **1966**, *108*, 1317. Guidon, Y.; Anderson, P. C. *Tetrahedron Lett.* **1987**, *28*, 2485. Guidon, Y.; Berstein, M. A.; Anderson, P. C. *Tetrahedron Lett.* **1987**, *28*, 2225. Gupta, R. B.; Franck, R. W. *J. Am. Chem. Soc.* **1987**, *109*, 6554.

(9) Mootoo, D. R.; Date, V.; Fraser-Reid, B. *J. Am. Chem. Soc.* **1988**, *110*, 2662.

(10) Ratcliffe, A. J.; Mootoo, D. R.; Andrews, C. W.; Fraser-Reid, B. *J. Am. Chem. Soc.* **1989**, *111*, 7661.

(11) Andrews, C. W.; Fraser-Reid, B.; Bowen, J. P. *J. Chem. Soc., Chem. Commun.* **1989**, 1913.

(12) Deslongchamps, P. *Stereoelectronic Effects in Organic Chemistry*; Pergamon Press: New York, 1983; p 30–35.

(13) (a) The *A* factor for CH_3 is 1.76 kcal, according to MM2. (b) See also: Eliel, E. L.; Hargrave, K. D.; Pietrusiewicz, K. M.; Manoharan, M. *J. Am. Chem. Soc.* **1982**, *104*, 3635.

(14) For a full dicussion of these conformations, see: Stoddard, J. F. *Stereochemistry of Carbohydrates*; Wiley-Interscience: New York, 1971; p 50–59.

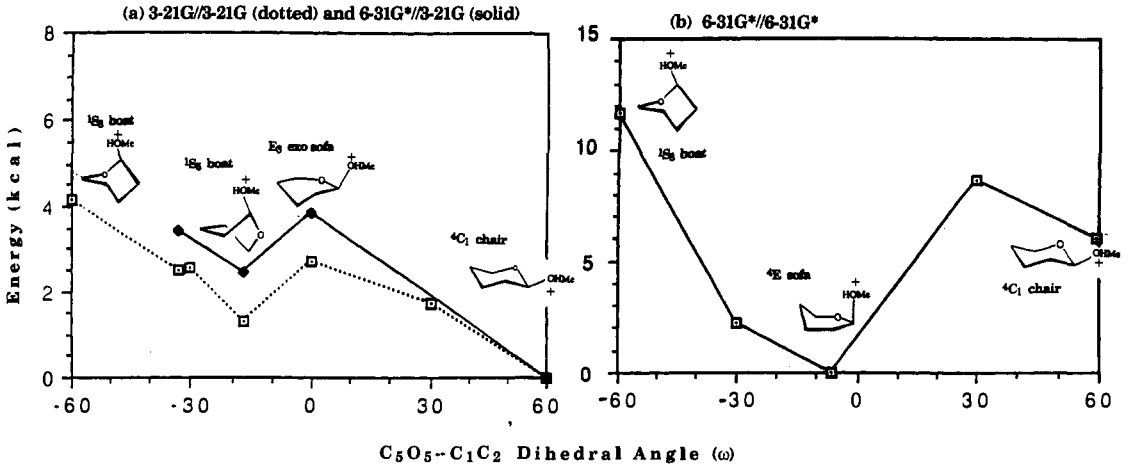

Figure 1. Chair–boat interconversion of protonated equatorial 2-methoxytetrahydropyran.

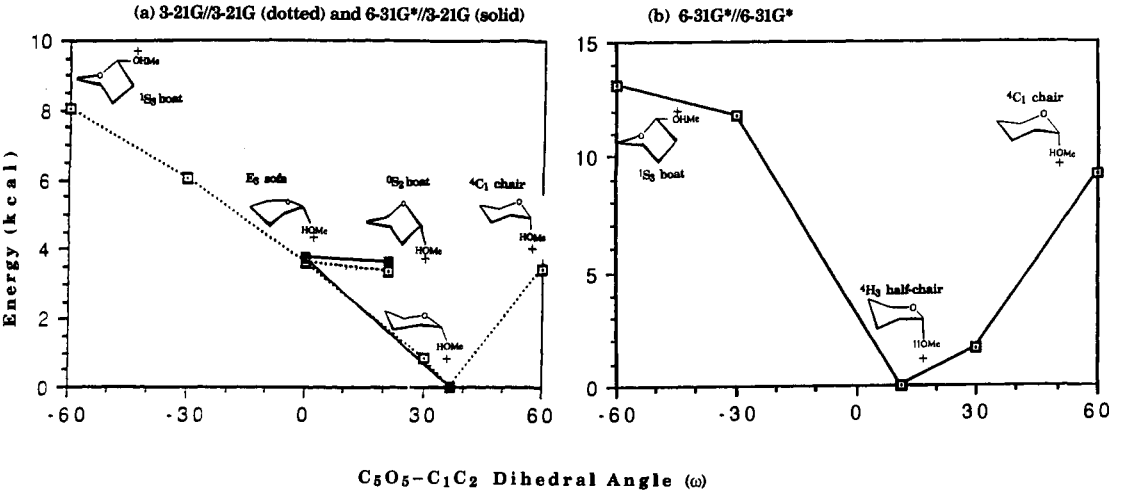

Figure 2. Chair–boat interconversion of protonated axial 2-methoxytetrahydropyran.

the lower energy, so the $^{1,4}B$ boat was eliminated. Indeed, the $^{1,4}B$ boat changes to the $^{1}S_3$ form during geometry optimization. For these reasons, the $^{1}S_5$ was chosen for $\omega = -30°$, and $^{1}S_3$ for $\omega = -60°$.

0° Conformers. Protonated methoxytetrahydropyrans (glycosides) with $\omega = 0°$ are geometrically related to the oxocarbenium ion **3** and therefore require special comment. To begin with, the 6-31G*//3-21G energies for the various conformations of the oxocarbenium ion **3** are shown in Scheme IV, part a. $^{4}H_3$ and ^{4}E are lowest in energy. Coplanarity of the C_5O_5–C_1C_2 domain means that the only centers that can pucker out of plane are *either or both* of C_3 and C_4. However, by applying criterion i, the $^{3}H_4$ and $^{2,5}B$ species can be ruled out, and since $B_{2,5}$ boats were rejected because of the flagpole interactions discussed in the preceding section (see Scheme III), we are left with the six structures shown in Scheme IV (parts b and c).

Sofas have only one carbon out of plane, and hence there are two conformationally allowed structures for each anomer, Scheme IV (parts b and c),[15] and these are interconvertible via $^{4}H_3$ half-chairs that have one carbon on either side of the plane.[16] (From the energies shown in Scheme IV (vide infra), it is seen that the protonated E_3 sofas are lower in energy than the corresponding ^{4}E counterparts with this basis set.)

Chair Conformations. The $^{4}C_1$ conformations ($\omega = +60°$) were chosen as the initial structures for both anomers in keeping with ample precedent.[17] Upon protonation of the exocyclic oxygen, conformational changes occurred. The structures lying between $\omega = +60°$ and 0° represent flattened chairs.

Selection of Protonated Transition-State Precursors

(a) 6-31G* Energies and 3-21G Geometries (6-31G*//3-21G). The above screening procedure provided us with one or more transition-state precursors for every value of ω. Energy profiles (E vs ω) were constructed after the lowest energy had been obtained at each point.

Our general operational strategy involved these stages: (1) the preferred conformations of the MeOTHP's were built with MacroModel,[18] constrained to the desired C_5O_5–C_1C_2 dihedral angle (i.e., value of ω), minimized by using the modified MM2 force field in MacroModel, and then protonated on O1;[19] (2) the geometries so obtained were optimized at the 3-21G level using Gaussian 86 and 88,[21] keeping the constraints in place; (3) where more than one alternative conformer was possible, the species with the lowest energy was chosen for use in the E vs ω plot, as was

(15) The symbol E indicates envelope conformation, the sub- or superscript indicates the out-of-plane atom, and endo and exo refer to the aglycon being on the same or opposite side of the plane.

(16) The $^{3}H_4$ half-chair is rejected because the C_5–CH_3OH residue would be pseudo axial.

(17) Kirby, A. J. *The Anomeric Effect and Related Stereoelectronic Effects at Oxygen*; Springer-Verlag: New York, 1983; Chapter 4 and references cited therein.

(18) Still, W. C.; Mohamadi, F.; Richards, G. T.; Guida, W. C.; Liskamp, R.; Lipton, M.; Caufield, C.; Chang, G.; Hendrickson, T. *MacroModel V 2.0*, Department of Chemistry, Columbia University, New York, NY 10027.

(19) The exoanomeric effect[20] was used to orient the methoxy group. The initial geometry about the protonated oxygen was planar and trigonal, and optimization would provide the lowest energy configuration for the protonated oxygen.

(20) Praly, J.-P.; Lemieux, R. U. *Can. J. Chem.* **1987**, *65*, 213.

(21) Frisch, M. J.; Binkley, J. S.; Schlegel, H. B.; Raghavachari, K.; Melius, C. F.; Martin, R. L.; Stewart, J. J. P.; Bobrowicz, F. W.; Rohlfing, C. M.; Kahn, L. R.; Defrees, D. J.; Seeger, R.; Whiteside, R. A.; Fox, D. J.; Fleuder, E. M.; Pople, J. A. Carnegie-Mellon Quantum Chemistry Publishing Unit, Pittsburgh, PA, 1984.

Scheme V. Progress from Protonated Intermediates to Transition States and Thence to Oxocarbenium Ions (6-31G*//3-21G)[a,b]

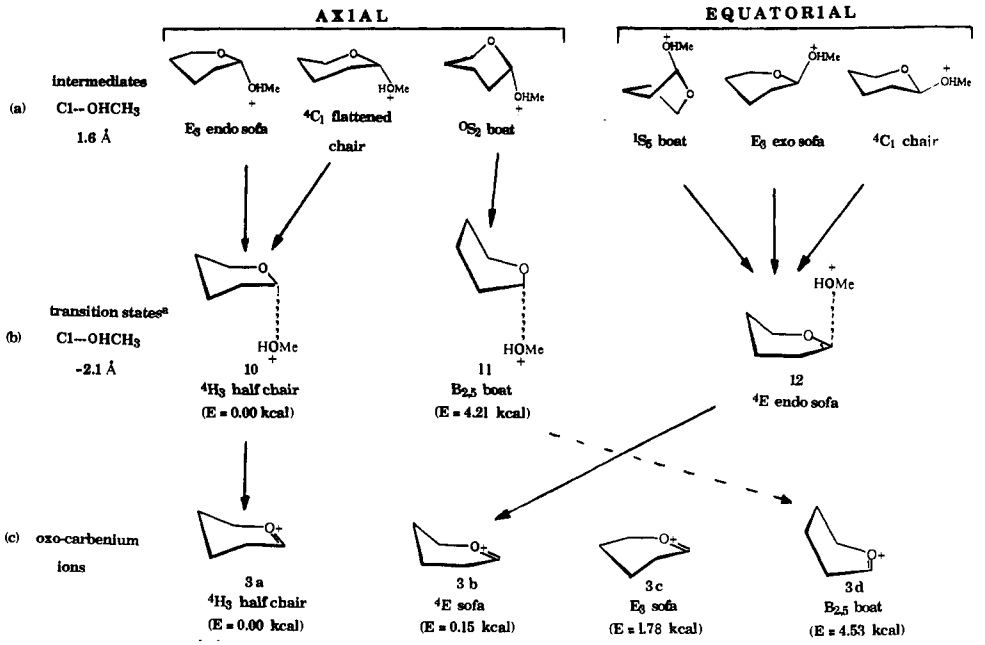

[a] Upon application of the 2.1-Å C_1–O_1 bond constraint, the E_3 species converts into ^4E. [b] The ^4E and E_3 ions interconvert through the $^4H_3$ species.

the case with the sofas in Scheme IV (parts b and c); and (4) the energies of preferred species were reevaluated with the 6-31G* basis set.

We therefore obtained energies *and* geometries for all values of ω at the lower level of theory (i.e., 3-21G//3-21G), but in order to construct better profiles for the dependence of energy on dihedral angle, *energies* were obtained at the (6-31G*//3-21G) level. Thus, from the two sets of curves shown in Figures 1a and 2a, the higher level results are seen to refine, although not substantially alter, the insight gained at the lower level.

For the equatorial anomer, Figure 1a, the $^4C_1$ chair is seen to be the global minimum, and the 0° conformer is the E_3 exo sofa. The plot indicated to us that the structure at −18° was a local minimum, corresponding to a $^1S_5$ boat (see Scheme III). Notably the $^1S_3$ boat itself at −60° (see Scheme II, **9c(H$^+$)**) is of higher energy.

Similar treatment of the axial anomer (Figure 2a) showed, surprisingly, that the global minimum was not the $^4C_1$ chair, but a structure at +37° that corresponds to a flattened chair. Further constraint of ω proceeds through the E_3 sofa (see Scheme IV) to the high-energy $^1S_3$ boat. *Note that the $^0S_2$ boat, which had been rejected in the above discussion on boat conformations, does not lie on the low-energy curve.* Nevertheless we decided to retain this conformer for future considerations (vide infra).

From Figures 1a and 2a, the most probable transition-state precursors can now be chosen on the basis of two criteria: (a) geometric, on the basis of ω = 0° dihedral angle, and (b) low energy.

Criterion a satisfies the least motion[22] requirement. Geometrically, the $^1S_5$ boat and E_3 exo sofa are clear choices for the equatorial anomer. On the basis of its low energy, we can also include the $^4C_1$ chair **9a(H$^+$)**.

With the axial anomer, the E_3 endo sofa is a clear choice on the basis of criterion a. The flattened $^4C_1$ chair (ω = +37°) conformer deserves consideration on the basis of criterion b.

What about the $^0S_2$ form at ω = +20°? It is related to both of the preferred axial conformations discussed in the preceding paragraph in that geometrically it is close to the flattened chair, and energetically it is identical with the E_3 sofa. Because the $^0S_2$ structure is close to the crucial ω = 0° mark, we decided to include it in spite of the fact that it had been rejected during the above conformational screening of boat conformations.

(22) Sinnott, M. L. *Adv. Phys. Org. Chem.* **1988**, *24*, 113.

Converging on the Transition States

The next stage of our study was to allow the six chosen intermediates to progress to the transition state(s). As indicated in Scheme V, mechanism a, the length of the C_1–OHMe bond for the five intermediates is ~1.6 Å after 3-21G optimization. For transition-state modeling, we chose a bond length of 2.1 Å for the C_1–OHMe bond,[23-25] and each chosen precursor was then reoptimized with this new constraint using the 3-21G basis set. In the case of the axial MeOTHP intermediates, the flattened chair and E_3 endo sofa went to the half-chair form **10** while the $^0S_2$ boat went to the $B_{2,5}$ boat **11** (Scheme V, mechanism b). *A profound difference for the equatorial MeOTHP is that the three intermediates all converged on the same transition state, the ^4E endo sofa **12**.*

The transition-state models **10–12** must now lose methanol to give the cyclic oxocarbenium ion, the various conformations of which are shown with associated energies in Scheme V, mechanism c. A most satisfying result is the correspondence between the geometries of low-energy protonated transition states and the low-energy cyclic ions (i.e., **10** with **3a**, and **12** with **3b**), which is in keeping with a late transition state in glycoside hydrolysis, a fact that has been established on the basis of kinetic investigations.[26]

Questions were raised above about the feasibility of the $^0S_2$ boat, both in the preliminary screening of boat conformations, and in our analysis of Figure 2. It transpires that our misgivings about the $^0S_2$ boat were well founded because from Scheme V it is seen to lead to high-energy structues **11** and **3d**.

(b) 6-31G* Energies and Transitions States (6-31G*//6-31G*). Although the foregoing 6-31G*//3-21G basis set was efficient at conformational searching and most revealing, we were concerned to obtain a better degree of refinement with respect to the nσ^* interaction, which is crucial to determining the most stable conformation of the ring by virtue of controlling the bond order

(23) Dorigo, A. E.; Houk, K. N. *Advances in Molecular Modeling*; JAI Press, Inc.: Greenwich, 1988; Vol. 1, p 135. Houk, K. N.; Tucker, J. A.; Dorigo, A. E. *Acc. Chem. Res.* **1990**, *23*, 101.

(24) Weiner, S. J.; Singh, C.; Kollman, P. A. *J. Am. Chem. Soc.* **1985**, *107*, 2219.

(25) Jorgensen, W. C.; et. al. Computer Simulation of Chemical and Biomolecular Systems. *Ann. N.Y. Acad. Sci.* **1986**, *482*, 198.

(26) For a recent study of transition-state structures based on kinetic isotope effects, see: Bennet, A. J.; Sinnott, M. L. *J. Am. Chem. Soc.* **1986**, *108*, 7287.

(27) A difference of 1.33 kcal was obtained by using 6-31G*//3-21G. Wiberg, K. B.; Murko, M. A. *J. Am. Chem. Soc.* **1989**, *111*, 4821.

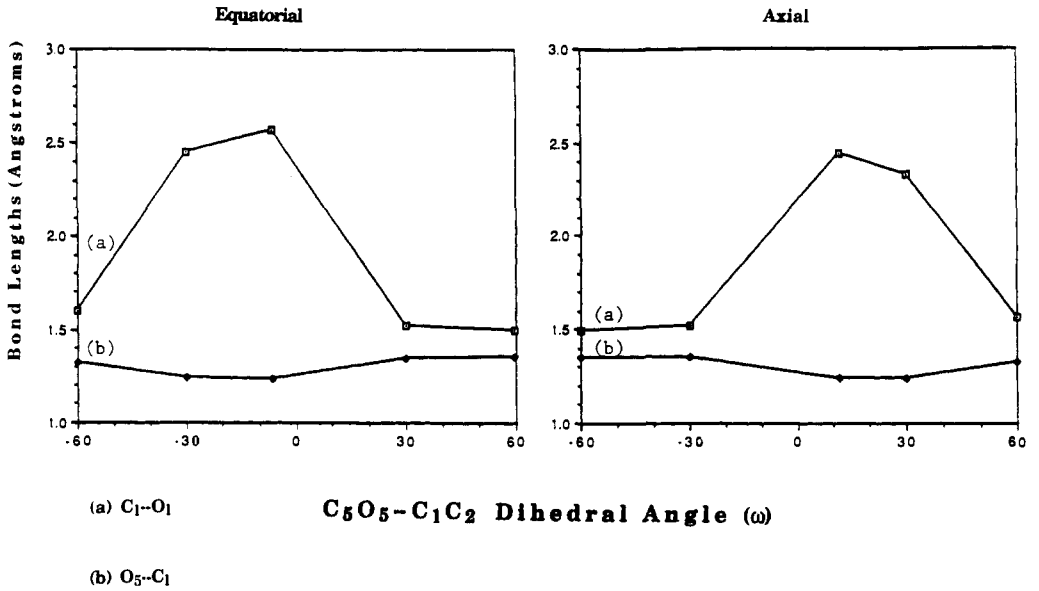

Figure 3. Correlated rehybridizations of endo and exo bonds at the anomeric center during exocyclic cleavage of protonated 2-methoxytetrahydropyrans (6-31G*).

of the O_5–C_1 bond. We therefore reoptimized the protonated glycosides in Figures 1a and 2a with the 6-31G* basis set, using constraints at each value of ω except at 0°, where each low-energy species was allowed to optimize fully. The low-energy species thus were fully characterized.

The advantage of the 6-31G* basis set is that hybridization is better represented, and hybridization of O_5 and C_1 is expected to change as a function of the degree of $n\sigma^*$ overlap.

The profiles shown in Figures 1b and 2b indicate some important differences from those in Figures 1a and 2a, respectively. Underlying the changes is the greater $n\sigma^*$ delocalization at the 6-31G* level of geometry optimization. In general, the global conformational minima observed in Figures 1b and 2b are shifted closer to $\omega = 0°$ and are deeper than before. $^4C_1$ chairs are no longer minima, and the E_3 sofas have been replaced by ^4E sofas.

Detailed comparison of the axial profiles (Figure 2) show that, with the better basis set, the low-energy species is a half-chair at $\omega = +11°$, which replaces the flattened chair at $\omega = +37°$.

The equatorial profiles, Figure 1, reveal even more profound differences. Thus, the global minimum is no longer the protonated chair at +60°, but is an ^4E sofa at −6°. The former is now relegated to a local minimum, a flattened chair at +30° being a conformational energy barrier.

The new minima at $\omega = +11°$ and $\omega = -6°$ are much more flattened in the C_5O_5–C_1C_2 region than before, reflecting a larger O_5–C_1 bond order.

Most satisfying, as revealed in Figure 3a,b, is the variation in the C_1–O_1 bond length (1.5–2.5 Å) as a function of ω. For both anomers, C_1–O_1 maximizes at ~2.5 Å, *without a bond length constraint*, well in excess of the 2.1-Å constraint used in the 3-21G studies to model the transition state. These maximum bond lengths occur in the minimum energy species. In addition, the maximum lengthening of the C_1–O_1 bonds correlates precisely with the maximum shortening of the O_5–C_1 bond (~1.23 Å), as a function of ω. These extreme values, 2.5 and 1.23 Å, when compared to the normal C–O bond length 1.4 Å, indicate that weakening of the bond to the protonated leaving group and double bond formation are well advanced in the $\omega = +11°$ and $\omega = -6°$ species. Thus, the minimum energy structures at $\omega = +11°$ and $\omega = -6°$ represent *late* transition-state models. These transition-state models are very similar to the 3-21G transition-state models **10** and **12**.

The observed correlations between the O_5–C_1 and C_1–O_1 bond lengths in both axial and equatorial anomers indicate that $n\sigma^*$ interactions are present in the transition state. This interaction will define the cleavage pathway in structural terms. It is obvious from Figure 3a,b that double bond formation (O_5–C_1) and bond breaking (C_1–O_1) occur concurrently with ring flattening (ω). Thus, the species that occur on the reaction coordinate at the point of cleavage are the half-chair, $^4H_3$, and sofa, ^4E, not chair or boat conformations.

Table I. β/α Rate Ratios for Hydrolysis of Some Methyl Pyranosides with 0.5 HCl at 75 °C[28]

glucose	1.9
2-deoxyglucose	2.5
tetra-*O*-methylglucose	2.5
mannose	2.4
galactose	1.8
xylose	2.0
rhamnose	2.3
arabinose	1.5

Scheme VI. Energetics of Cleavage of 2-Methoxytetrahydropyran Anomers (6-31G*//6-31G*)[a]

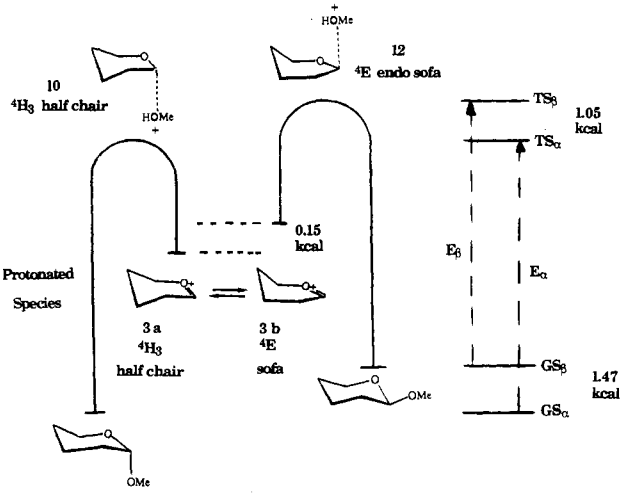

[a] $E_\beta + 1.47 = E_\alpha + 1.05$, $E_\alpha - E_\beta = 1.47 - 1.05 = 0.42$ kcal, $k_\beta/k_\alpha = \exp(-(E_\beta - E_\alpha))/RT = \exp(E_\alpha - E_\beta)/RT$).

Verifying the Validity of Transition States

Experimentally, the rate ratio for a wide variety of equatorial and axial anomers is ~2:1 in favor of the former, irrespective of the C_2–C_4 configurations (Table I). The ratio therefore un-

(28) Isbell, H. S.; Frush, H. L. *J. Res. Natl. Bur. Std. (U.S.)* **1940**, *24*, 125.

doubtedly reflects a fundamental internal energy difference related to the anomeric stereochemistry. We have sought to use the calculated transition-state energies to demonstrate this.

The analysis in Figures 1 and 2 can be conveniently summarized as shown in Scheme VI, and this display suggests a method for testing the validity of the entire investigation. We have determined the energy difference between the transition-state strctures **10** and **11** to be 1.05 kcal (6-31G*//6-31G*, Scheme VI). The difference in ground-state energies for glycosides **8** and **9** has been found by us to be 1,47 kcal (6-31G*//6-31G*).[27] On the assumption that entropies and solvation energies are the same for the α and β anomers, the Arrhenius equation can be applied as shown in Scheme VI to compare relative rate constants for axial and equatorial cleavage—assuming that the preexponential factors are equal. For a temperature of 75 °C, the above treatment predicts that β/α rate ratio should be 1.8 and is therefore in good agreement with the data in Table I. For a temperature of 23 °C, the predicted ratio is 1.9, and this agrees with the value of 2.0 obtained for the restrained anomers studied by us.[10]

The good agreement between calculated and observed rate constants suggests that our transition-state analyses are credible and, by corollary, that the transition-state structures in hydrolysis of axial and equatorial glycosides are $^4H_3$ and ^4E, respectively. Our results offer more refined conformational analysis than that obtained in the elegant kinetics studies of Bennet and Sinnott.[27] That $n\sigma^*$ interactions play a profound role in oxygen basicities[11] and bond reorganizations is apparent from our studies. A full investigation of these effects and their roles in competing reaction pathways, e.g., endo vs exo glycoside cleavage, is underway and will be reported in due course.

Acknowledgment. This work was supported by grants from the National Science Foundation (CHE 8703916) and National Institutes of Health (GM-41071) to B.F.-R. and from the North Carolina Supercomputing Center to B.F.-R., J.P.B., and C.W.A. We thank the Biological Instrumentation Program (NSF) for use of the Convex C220 at the University of North Carolina, Chapel Hill.

Registry No. 3, 72036-48-7; 8 (H^+), 135789-43-4; 9 (H^+), 135789-44-5.

(29) See for example: Hough, L.; Richardson, A. C. In *Comprehensive Organic Chemistry*; Ed. Barton, D., Ollis, W. D., Eds.; Pergamon: Oxford, 1974; Vol. V, p 692. For the alternative usage, see *Principles of Organic Stereochemistry*; Testa, B. Ed.; Dekker: New York, 1979; p 86.

Optical Activity Arising from ^{13}C Substitution: Vibrational Circular Dichroism Study of (2*S*,3*S*)-Cyclopropane-*1*-^{13}C,^2H-*2*,*3*-$^2H_2$

Teresa B. Freedman,* Steven J. Cianciosi, N. Ragunathan, John E. Baldwin, and Laurence A. Nafie

Contribution from the Department of Chemistry, Syracuse University, Syracuse, New York 13244-4100. *Received January 18, 1991*

Abstract: Vibrational circular dichroism (VCD) spectra of the novel chiral compound (2*S*,3*S*)-cyclopropane-*1*-^{13}C,^2H-*2*,*3*-$^2H_2$ (**1**) are reported. This quadruply labeled cyclopropane is chiral due to substitution of ^{13}C at carbon 1 of *anti*-cyclopropane-*1*,*2*,*3*-$^2H_3$ (**2**). In C_2Cl_4 solution, a conservative (+,−,+) VCD pattern is observed in both the CH and CD stretching regions. From normal-coordinate analysis, these VCD bands are found to arise from chiral perturbation which mixes the A′ and A″ symmetry modes of **2**. Excellent quantitative agreement with the experimental VCD spectra is obtained by applying a generalized coupled-oscillator model to the motions of the two pairs of chirally oriented trans CH or CD oscillators.

Introduction

Chirality can be introduced into a nondissymmetric molecule by nuclear isotopic substitution that makes it dissymmetric by eliminating reflection, inversion, or, more generally, S_n symmetry. Several molecules that are chiral due to deuterium substitution have been investigated[1-8] by vibrational circular dichroism (VCD) spectroscopy.[9-13] In these cases, the heavier mass of the deuterium causes an ~800-cm^{-1} decrease in the CH stretching frequency and significant shifts in the CH bending frequencies as well, resulting in modes in which the CH and CD motions are largely uncoupled from each other. The VCD bands, in most cases, can be attributed to the coupled motion of chirally oriented CH or CD oscillators.[2-6]

Substitution of ^{13}C for ^{12}C results in an ~9-cm^{-1} decrease in the CH stretching frequency, an ~7-cm^{-1} decrease in the fre-

(1) Polavarapu, P. L.; Nafie, L. A.; Benner, S. A.; Morton, T. H. *J. Am. Chem. Soc.* **1981**, *103*, 5349.
(2) Annamalai, A.; Keiderling, T. A.; Chickos, J. S. *J. Am. Chem. Soc.* **1984**, *106*, 6254.
(3) Annamalai, A.; Keiderling, T. A.; Chickos, J. S. *J. Am. Chem. Soc.* **1985**, *107*, 2285.
(4) Freedman, T. B.; Paterlini, M. G.; Lee, N.-S.; Nafie, L. A.; Schwab, J. M.; Ray, T. *J. Am. Chem. Soc.* **1987**, *109*, 4727.
(5) Cianciosi, S. J.; Spencer, K. M.; Freedman, T. B.; Nafie, L. A.; Baldwin, J. E. *J. Am. Chem. Soc.* **1989**, *111*, 1913.
(6) Freedman, T. B.; Spencer, K. M.; McCarthy, C.; Cianciosi, S. J.; Baldwin, J. E.; Nafie, L. A.; Moore, J. A.; Schwab, J. M. *Proc. SPIE-Int. Soc. Opt. Eng.* **1989**, *1145*, 273.
(7) Spencer, K. M.; Cianciosi, S. J.; Baldwin, J. E.; Freedman, T. B.; Nafie, L. A. *Appl. Spectrosc.* **1990**, *44*, 235.
(8) Cianciosi, S. J.; Ragunathan, N.; Freedman, T. B.; Nafie, L. A.; Baldwin, J. E. *J. Am. Chem. Soc.* **1990**, *112*, 8204.
(9) Freedman, T. B.; Nafie, L. A. In *Topics in Stereochemistry*; Eliel, E., Wilen, S., Eds.; Wiley: New York, 1987; Vol. 17, pp 113-206.
(10) Stephens, P. J.; Lowe, M. A. *Annu. Rev. Phys. Chem.* **1985**, *36*, 213.
(11) Keiderling, T. A. In *Practical Fourier Transform Infrared Spectroscopy*; Ferraro, J. R., Krishnan, K., Eds.; Academic Press: San Diego, CA, 1990; pp 203-283.
(12) Polavarapu, P. L. In *Vibrational Spectra and Structure*; Durig, J. R., Ed.; Elsevier: Amsterdam, 1984; Vol. 13, pp 103-160.
(13) Nafie, L. A. In *Advances in Infrared and Raman Spectroscopy*; Clark, R. J. M., Hester, R. E., Eds.; Wiley-Heyden: London, 1984; Vol. 11, p 49.

0002-7863/91/1513-8298$02.50/0